Revista Brasileira de Ciência do Solo

Division - Soil Use and Management | Commission - Soil and Water Management and Conservation

Spatial Distribution of Annual and Monthly Rainfall Erosivity in the Jaguarí River Basin

Lucas Machado Pontes[(1)], Marx Leandro Naves Silva[(1)*], Diêgo Faustolo Alves Bispo[(1)], Fabio Arnaldo Pomar Avalos[(1)], Marcelo Silva de Oliveira[(2)] and Humberto Ribeiro da Rocha[(3)]

[(1)] Universidade Federal de Lavras, Departamento de Ciência do Solo, Lavras, Minas Gerais, Brasil.
[(2)] Universidade Federal de Lavras, Departamento de Ciências Exatas, Lavras, Minas Gerais, Brasil.
[(3)] Universidade de São Paulo, Instituto de Astronomia Geofísica e Ciências Atmosféricas, Departamento de Ciências Atmosféricas, São Paulo, São Paulo, Brasil.

ABSTRACT: The Jaguarí River Basin forms the main water supply sources for the São Paulo Metropolitan Region and other cities in the state. Since the kinetic energy of rainfall is the driving force of water erosion, the main cause of land and water degradation, we tested the hypothesis of correlation between the erosive potential of rainfall (erosivity) and geographical coordinates and altitude for the purpose of predicting the spatial and temporal distribution of the rainfall erosivity index (EI_{30}) in the basin. An equation was used to estimate the (EI_{30}) in accordance with the average monthly and total annual rainfall at rainfall stations with data available for the study area. In the regression kriging technique, the deterministic part was modeled using multiple linear regression between the dependent variable (EI_{30}) and environmental predictor variables: latitude, longitude, and altitude. From the result of equations and the maps generated, a direct correlation between erosivity and altitude could be observed. Erosivity has a markedly seasonal behavior in accordance with the rainy season from October to March. This season concentrates 86 % of the estimated EI_{30} values, with monthly maximum values of up to 2,342 MJ mm ha^{-1} h^{-1} $month^{-1}$ between December and January, and minimum of 34 MJ mm ha^{-1} h^{-1} $month^{-1}$ in August. The highest values were found in the Mantiqueira Range region (annual average of up to 12,000 MJ mm ha^{-1} h^{-1}), a region that should be prioritized in soil and water conservation efforts. From this validation, good precision and accuracy of the model was observed for the long period of the annual average, which is the main factor used in soil loss prediction models.

Keywords: geostatistics, soil and water conservation, erosion, EI_{30}.

*** Corresponding author:**
E-mail: marx@dcs.ufla.br

Received: September 15, 2016
Approved: April 18, 2017

How to cite: Pontes LM, Silva MLN, Bispo DFA, Avalos FAP, Oliveira MS, Rocha HR. Spatial distribution of annual and monthly rainfall erosivity in the Jaguarí River Basin. Rev Bras Cienc Solo. 2017;41:e0160407.
https://doi.org/10.1590/18069657rbcs20160407

INTRODUCTION

The Jaguarí River Basin has a drainage area that forms the main sources of water supply for the metropolitan areas of the state of São Paulo, such as the Cantareira System and the Piracicaba River. Due to the severe drought in 2013 and 2014 in the southeast region of Brazil (Coelho et al., 2016), the issue of water security has gained even more relevance in these regions. However, the problems of land use and occupation historically and continuously threaten the quality of surface water, the useful life of reservoirs, and the productive capacity of the soil, and the greatest cause of degradation is water erosion (Telles et al., 2011). Effective control of erosive processes in river basins depends on studies of the spatial and temporal behavior of erosive factors, especially rainfall erosivity (Martins et al., 2010; Silva et al., 2010).

The kinetic energy of rainfall is the driving force of water erosion, with a direct effect on detachment of soil particles, breaking the aggregates and transporting particles through surface runoff (Wischmeier and Smith, 1978; Panagos et al., 2015). Wischmeier (1959) proposed the EI_{30}, which relates the kinetic energy to the maximum intensity in 30 minutes of rain events, to represent the erosivity or erosive potential of the rains.

Traditionally, the EI_{30} is estimated through rainfall data with a minimum temporal resolution of 30 minutes, but historical series with this information are rare and, therefore, alternative approaches have been used. Equations that relate monthly and annual total rainfall data with the EI_{30} generated for locations with data availability allow the use of 24-hour resolution information, which is easier to access and to estimate erosivity in adjacent locations (Renard et al., 1997; Silva, 2004; Oliveira et al., 2012).

The spatial distribution of erosivity in river basins is indispensable information for modeling critical scenarios in conservation planning and in adoption of soil and water conservation practices on this scale (Martins et al., 2010). Studies demonstrated that geostatistical techniques have an advantage over traditional interpolators in the spatialization of environmental data (Hengl et al., 2007; Akkala et al., 2010) because the prediction model is composed of a deterministic part (overall average) and a stochastic part, provided by spatial autocorrelation, in order to obtain the Best Linear Unbiased Prediction (BLUP) (Hengl, 2007).

In regression kriging (RK), the deterministic part of spatial variance is obtained externally, with a regression model between the response variable and environmental factors as predictor variables (Hengl, 2007; Lark, 2012). These predictor variables should preferably be easy to obtain and have a better spatial distribution than the variable to be estimated. The rainfall and erosivity show correlation with continental (coordinate) and topographic (altitude) properties (Meusburger et al., 2012; Mello et al., 2013; Panagos et al., 2015), which can be used in the regression model. These properties are easily acquired through remote sensing images.

The use of regression methods combined with geostatistical methods has shown good results for large regions with complex atmospheric conditions and a limited sampling network. Meusburger et al. (2012) used regression kriging to estimate the monthly erosivity average in Switzerland and obtained rainfall regression models with a determination coefficient of 0.68 and 0.76. Mello et al. (2013), in a study regarding annual erosivity in Brazil using regression kriging, used latitude, longitude, and altitude and their 2nd and 3rd order terms to predict erosivity and obtained equations with up to 18 terms, with a coefficient of determination above 0.68 in all cases.

Studies of erosivity mapping on a national scale (Silva, 2004; Oliveira et al., 2012; Mello et al., 2013) and for the states of Minas Gerais (Mello et al., 2007; Moreira et al., 2008), with specific details for the south of the state of Minas Gerais (Aquino et al., 2012), and São Paulo (Vieira and Lombardi Neto, 1995; Moreira et al., 2006) showed analysis on a regional scale with low spatial resolution. However, river basins are the basic unit of planning and management of water resources, and the planning and implementation of soil and water conservation practices require a level of spatial detail consistent with their scale (Silva et al., 2010).

The hypothesis of correlation between the erosive potential of rainfall (erosivity) and geographical coordinates together with altitude was tested. The objective of this study was to present a technique to determine spatial prediction from measures of precision and accuracy and the seasonal rainfall erosivity standard, using the EI_{30}, for use in studies that seek to identify the areas most susceptible to erosion in the Jaguarí River Basin.

MATERIALS AND METHODS

Study Area

The study covers the Jaguarí River Basin, with a drainage area of 4,320 km^2, of which 74 % are in the state of São Paulo and the highest part, with 1,140.80 km^2, in the state of Minas Gerais (Figure 1).

The climate in the basin is humid subtropical (C) and was divided into four classes, according to the Köppen classification system. The Mantiqueira Range region has a Cwb climate (dry winter and temperate summer); the Jaguari middle region has a Cfb climate (temperate summer and no dry season); and the lower part of the basin has Cwa (dry winter and hot summer) and Cfa (hot summer and no dry season) classes (Alvares et al., 2013). The average annual rainfall in the basin is 1,488 mm, with more than 70 % concentrated in the rainy period from October to March.

Estimation of erosivity

The EI_{30}, which correlates kinetic energy with the maximum intensity of rainfall in 30 minutes, was used to represent the rainfall erosivity. Originally, this index was calculated by equations proposed by Wischmeier and Smith (1978). However, due to the scarcity of adequate historical rainfall series, erosivity has been estimated by equations

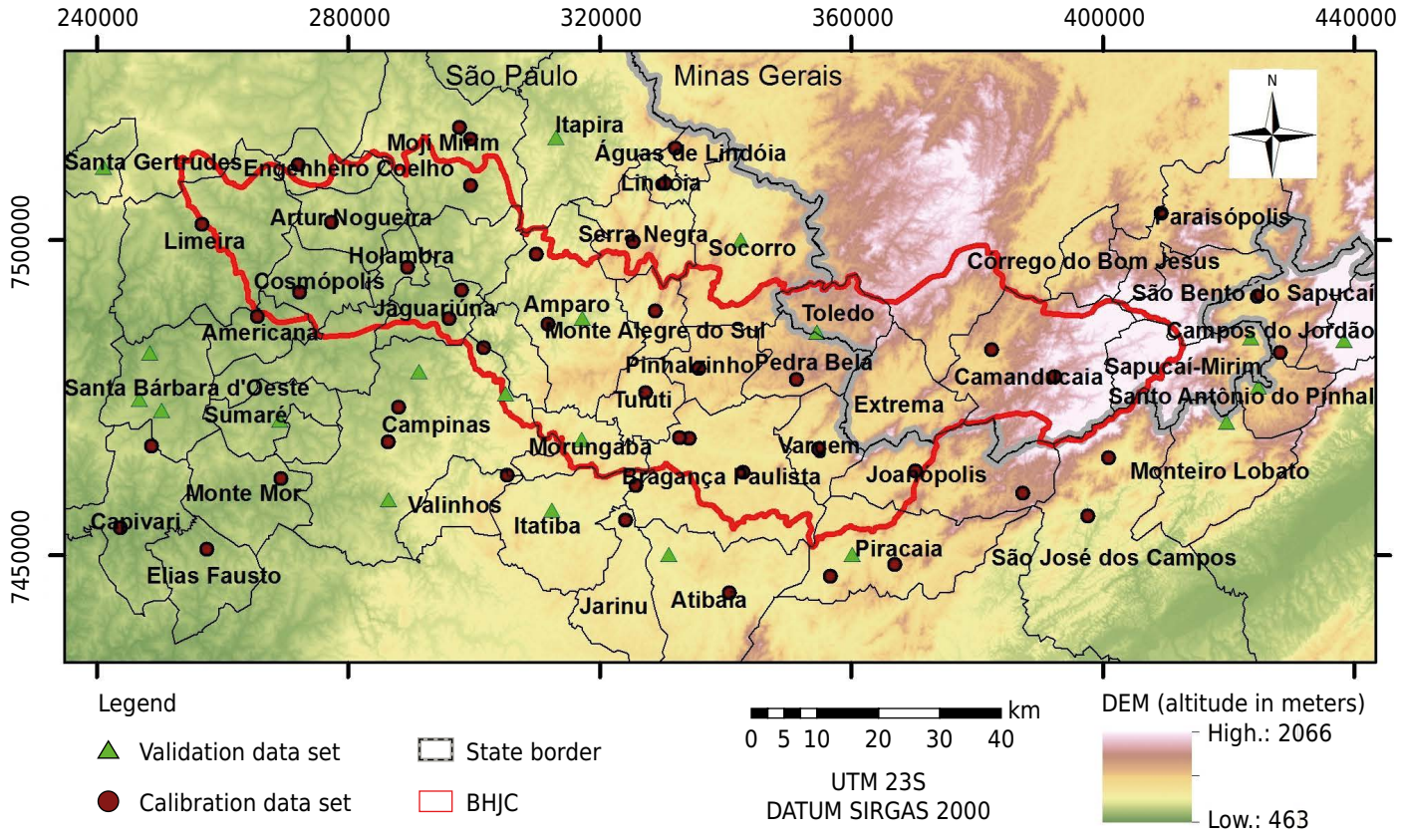

Figure 1. Jaguarí River Basin digital elevation model (DEM) and the rain gauge station locations and municipalities. DEM data: 90 m spatial resolution SRTM image between coordinates -23.24° and -22.31° S and 47.74° and 45.39° W.

that relate the EI_{30} to monthly rainfall values and annual rainfall (Oliveira et al., 2012). In this study, the equation 1, obtained for the region of Campinas, São Paulo (Lombardi Neto and Moldenhauer, 1992) was used:

$$EI_{30} = 68.730\ (p^2/P)^{0.841} \quad \text{Eq. 1}$$

in which the EI_{30} is the index that represents rainfall erosivity in MJ mm ha^{-1} h^{-1}; p is the total monthly rainfall in mm; and P is the annual rainfall in mm. The choice of this equation was based on the proximity to the study region and because of the absence of data with the necessary temporal resolution for direct calculation of the EI_{30} in the rain gauge stations located in the hydrographic basin.

In addition, the precipitation concentration index (PCI) (Oliver, 1980), used to select the EI_{30} equations most suitable for a local data set, indicated that the data of the rain gauge stations of the basin show a monthly distribution similar to that observed in Campinas, SP. The correlation between the monthly rainfall data of the Campinas station with those of the other stations used in the study showed a correlation coefficient always above 0.94.

The data of the rain gauge stations used were those of the National Water Agency (*Agência Nacional de* Águas). Double mass analysis was carried out to evaluate the consistency of the data, and the Spearmann and Mann-Kendall statistical tests were applied to verify trends. Thus, 66 rain gauge stations were selected (Figure 1) with stationary and consistent data for the period from 1970 to 2010. Some stations do not have information for the entire period, and in these cases, the largest available series was used, with stations with less than 20 consecutive years of data being discarded within the period mentioned.

The monthly and annual totals were calculated from the daily data, and the monthly gaps were filled using the Weighted Regionalization method. After that, the rainfall averages were reevaluated for each month, as well as the annual total, with which the EI_{30} was calculated, according to equation 1.

Regression Kriging

Spatial prediction of erosivity values using the EI_{30} was carried out using the technique known as regression kriging (RK) (Hengl et al., 2004; Hengl et al., 2007). In this study, this technique was divided into three main steps: principal component analysis, stepwise multiple linear regression, and kriging of the residues.

Principal component analysis (PCA) was carried out for the altitude (DEM), latitude, and longitude variables used to solve the multiple collinearity problem (Hengl et al., 2003; Panagos et al., 2014). The three variables were normalized before being used in the PCA, for which the average of each variable was subtracted from the respective original data and then divided by its standard deviation.

Stepwise multiple linear regression was adjusted between the major components (eigenvectors) and the EI_{30} monthly values and annual average. In this step, a random sampling of the stations was carried out, of which 46 (70 %) were used in the regression (calibration samples) and the rest (20 stations) were used to validate the predicted values with RK. The PCA and the regression were performed with the SAGA GIS 2.1.4 program (Conrad et al., 2015). The use of the 2nd and 3rd order terms in the PCA and in the regression was tested, but because they did not show improvement in the coefficient of determination (R^2), the simpler model was chosen.

The difference between the EI_{30} values observed in the calibration stations and the values estimated by the regression was calculated for each rainfall station used in the regression, constituting the regression error or residue. These residues were spatialized by ordinary kriging and then added to the regression result, which characterizes the method known as regression kriging (Hengl et al., 2004). The sum of the regression surface with spatialized errors by kriging resulted in maps of the spatial distribution of erosivity.

For kriging of the residues, the spherical, Gaussian, potential, and exponential semivariogram models were tested, adjusted by minimization of the residual square sum (RSS) of the geoR (Ribeiro Junior and Diggle, 2015). The adjusted semivariogram model was selected according to external validation; the models with the lowest average error were selected.

External validation was performed with data from 20 randomly selected stations, as mentioned above, so these data were not used in the regression and kriging steps. After generating the regression kriging results, the data from the external validation stations were used to calculate the average error (ME) according to equation 2:

$$ME = \frac{1}{n} \Sigma_{i=1}^{n} Z(x_i) - \hat{Z}(x_i) \quad \text{Eq. 2}$$

in which n is the number of stations used in the external validation (20); $Z(x_i)$ is the erosivity data observed at point x_i; and $\hat{Z}(x_i)$ is the erosivity value predicted by Kriging at point x_i. The average error is used as a measure of precision, so the t test was performed to verify if the ME was null at the significance level of 5 %. To evaluate the accuracy, the mean squared deviation ratio (MSDR) was used according to equation 3:

$$MSDR = \frac{1}{n} \Sigma_{i=1}^{n} \frac{\{Z(x_i) - \hat{Z}(x_i)\}^2}{\hat{\sigma}_k^2(x_i)} \quad \text{Eq. 3}$$

in which $\hat{\sigma}_k^2(x_i)$ is the variance of kriging, and the other terms are the same as those indicated above. Ideally, the ME is zero, and the MSDR should be equal to or close to 1 (Oliver and Webster, 2014).

RESULTS AND DISCUSSION

The monthly average rainfall and estimated erosivity of the 66 rainfall stations used are shown in figure 2.

The region is characterized by climatic seasonality, with a predominance of dry winter and rainy summer, which directly influences the seasonal distribution of erosivity. This characteristic is common to all the rainfall stations used in this study, which justifies the use of only one equation to estimate the erosivity index (EI_{30}) in accordance with the average monthly rainfall (Michiels et al., 1992).

Longitude and altitude showed a moderate correlation (0.57); that is, the altitude increases from west to east in the basin. Thus, it is important to avoid collinearity to adjust stepwise regression; otherwise, altitude could be disregarded and only the geographic coordinates (latitude and longitude) would be used to predict erosivity.

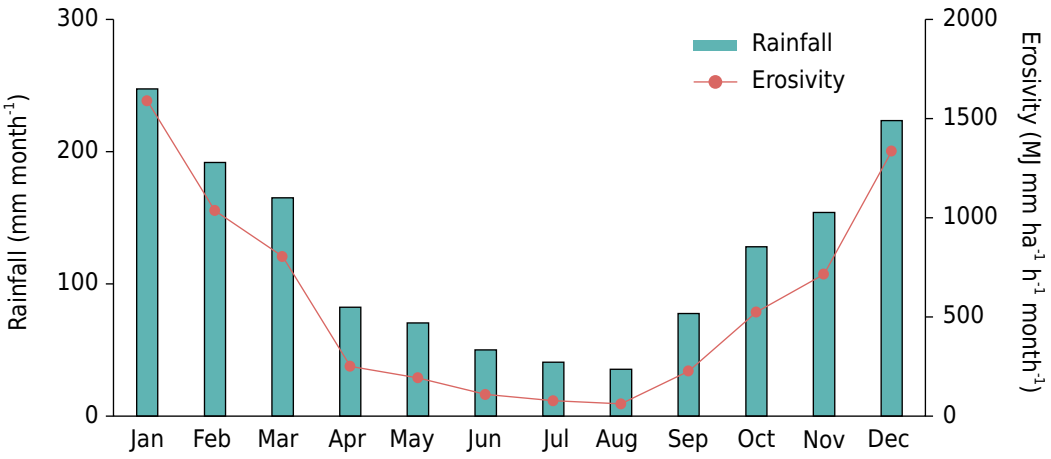

Figure 2. Monthly means of rainfall and erosivity data from 1970 to 2010 for the 66 rain gauge stations used in regression kriging.

Thus, PCA between the coordinates and the altitude results in components orthogonal to each other, in which the variables appear independently combined, which allows multiple regression to be adjusted without the bias of multiple collinearity. The principal components (PCA) of the altitude, latitude, and longitude variables, with the explained variance, eigenvalues, and eigenvectors, are shown in table 1.

The eigenvectors are the multiplier weights of each original variable (altitude, latitude, and longitude) used to obtain each PC (principal component), which are then used in stepwise regression. The eigenvalues provide the amount of variance explained by the respective component, such that PC1 has the highest eigenvalue, PC2 the second highest, and so on.

Component 1 is a combination of the three variables explaining 54 % of the variance. Component 2, which explains 33 % of the variance, is given by a combination between latitude and longitude. Together, components 1 and 2 explained 87 % of the variance and, therefore, obtained significant angular coefficients in stepwise regression (Table 2).

The EI_{30} values estimated by the regression are given by the sum of the intercept with the angular coefficients multiplied by the eigenvector of the principal components.

The results of stepwise multiple linear regression obtained intercepts, angular coefficients, and coefficient of determination (R^2) at a significance level of 5 % (Table 2). The coefficient of determination (R^2) showed values greater than 40 % for the months of October, December, April, August, and September and for the annual average. The months of January, March, and June showed R^2 lower than 20 %, but all significant at the 5 % level.

Table 1. Results of principal component analysis (PCA) on elevation, latitude, and longitude

PC	Cumulative Variance	Eigenvalue	Eigenvector		
			Elevation	Latitude	Longitude
	%				
1	53.70	1.611	-0.358078	-0.660220	-0.660220
2	87.03	1.000	0.000000	0.707107	-0.707107
3	100	0.389	0.933692	-0.253199	-0.253199

PC: principal component.

Table 2. Results of multiple linear regression (intercept and coefficients) between rainfall erosivity and principal components (PC)

Period	Coefficient*				Adjusted R^2	F-statistic
	Intercept	PC1	PC2	PC3		F; p-value
Annual	7867.5	95.4	-	-	49.4	44.9; 3.1×10^{-8}
Oct	615.1	97.2	-	-	46.1	39.5; 1.3×10^{-7}
Nov	823.0	112.6	-	-	33.1	23.3; 1.7×10^{-5}
Dec	1505.3	187.5	-90.3	-	44.9	19.3; 1.0×10^{-6}
Jan	1717.5	120.6	-	-	18.7	11.3; 0.002
Feb	1159.2	136.8	-	-	24.8	15.9; 0.0002
Mar	917.4	110.9	-	-	19.0	11.6; 0.001
Apr	310.3	72.5	-	-	45.7	38.9; 1.5×10^{-7}
May	231.2	25.8	20.5	-	32.6	11.9; 7.9×10^{-5}
Jun	131.8	-4.9	-	-	11.0	6.6; 0.01
Jul	96.4	12.0	18.3	-	34.1	12.6; 4.8×10^{-5}
Aug	80.8	17.0	12.7	-	42.1	17.4; 3.0×10^{-6}
Sep	280.3	50.4	33.3	-	49.5	23.0; 1.6×10^{-7}

* Significant intercepts and coefficients ($p<0.05$).

The coefficient of determination indicates the spatial variation of erosivity explained only with the regression models, that is, how much of this variation is due to the spatial trend. The difference between the values estimated by the regression and the values obtained for the calibration stations constitute the errors or residues. The residues preserve only the structure of the spatial autocorrelation of this phenomenon since the trend was withdrawn in the regression step. Thus, the errors were spatialized through the ordinary kriging, according to the study of the semivariogram for each period (Figure 3 and Table 3).

For the months with the low rainfall rates, May and June, the experimental semivariograms did not show a defined structure, characterizing the pure nugget effect (Table 3).

The pure nugget effect model, adjusted for the months of May and June, shows only the value of the C_0 parameter (nugget), constant for the entire sampling area. This can be explained by the low rainfall in these months throughout the basin, which may bring about a low spatial correlation for erosivity due to the randomness of the process.

For the other months, Gaussian, spherical, and exponential models were adjusted, for which the threshold values ($C_0 + C_1$) were close to the overall variance of the erosivity data, as expected.

The range of the adjusted models was from 12.33 km (July) to 159.08 km (August). Thus, the minimum spacing between stations should be 12 km so that the spatial distribution effect of rainfall and erosivity can be detected in semivariogram studies. The average range for the monthly semivariograms was 72.67 km, similar to that found by Vieira and Lombardi Neto (1995) for the state of São Paulo (70 km).

For the annual average, the semivariogram model was of the potential type, characterized by not having a defined threshold. Therefore, the A and C_1 parameters cannot be interpreted as reach and contribution as in the other models. In this case, A and C_1 are the exponent and the angular coefficient of the potential equation, respectively (Equation 4).

$$\gamma(h) = C_0 + C_1 \times h^A \quad \text{Eq. 4}$$

in which $C_1 > 0$, $0 < A < 2$.

These situations can be explained by the phenomenon of infinite dispersion, or by the area of study being smaller than the reach of the spatial dependence of the process, or by insufficient sampling of the area (Oliver and Webster, 2014).

Concerning the number of sampling locations, in the Mantiqueira Range region, there are only two stations with data available and that were used in the study, and only one of them, the Ponte Nova station, at 1,300 m altitude, is inside the basin. The Campos de Jordão station, located at 1,642 m altitude, is outside the limits of the basin. Therefore, in areas of higher altitude, the sampling is poor, which increases the uncertainties involved in modeling and results in larger errors in these areas (Mello and Silva, 2009).

The use of the erosivity regression model in accordance with altitude provides a measure of information that complements, even if in small degree, the lack of sampling at higher altitudes. However, the existence of this regression does not make better sampling in these sub-sampled regions unnecessary. The existence of a regression model between erosivity and altitude is corroborated by the fact that the increase in altitude from west to east leads to an increase in rainfall and erosivity in the same direction.

Regarding temporal variation, the results of external validation (Table 4), allow us to ascertain the quality of the predicted EI_{30} values.

With the exception of October, where there is a significant overestimation of the EI_{30}, the average error of the external validation results was not significantly different from zero at the 5 % level in most months, which suggests a satisfactory adjustment. Yet, in general, the

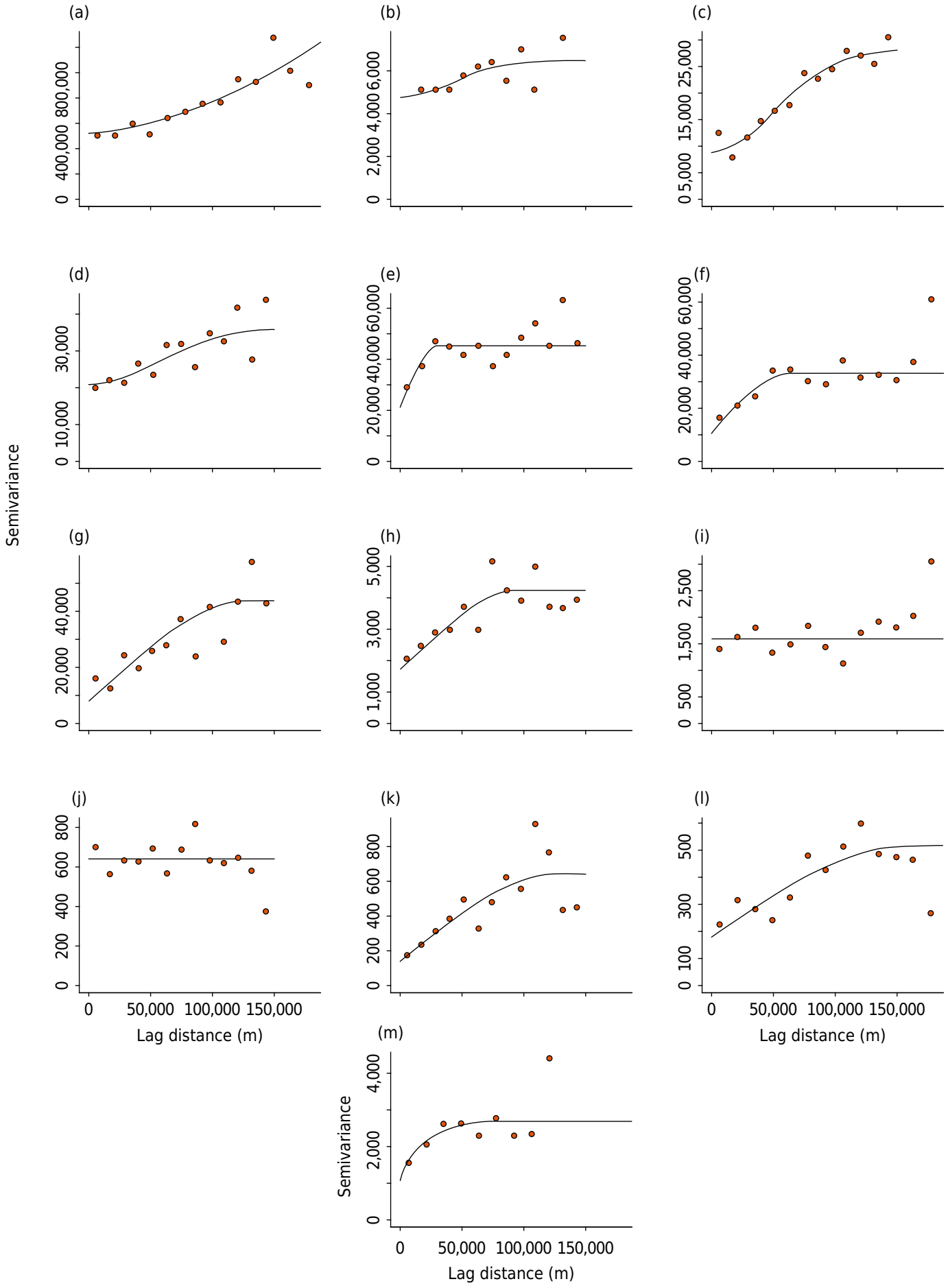

Figure 3. Residual semivariograms for the annual mean (a), and for the months of October (b), November (c), December (d), January (e), February (f), March (g), April (h), May (i), June (j), July (k), August (l), and September (m).

Table 3. Parameters of models fitted to experimental semivariograms of rainfall erosivity

Period	Model[(1)]	R	C_0	C_1	$C_0 + C_1$
Annual	Pow	1.689	517067.2	0.000907	-
Oct	Gau	58200.68	4779.538	1681.449	6460.987
Nov	Gau	72845.41	8715.848	19317.02	28032.87
Dec	Gau	77429.81	20992.01	15182.7	36174.7
Jan	Sph	31188.34	21292.64	24036.55	45329.19
Feb	Sph	65150.29	11101.72	23682.92	34784.64
Mar	Sph	131592.7	7721.69	35431.09	43152.78
Apr	Sph	98422.44	1719.88	2513.15	4233.03
May	Nugget	0	1588.554	0	-
Jun	Nugget	0	643.3894	0	-
Jul	Sph	12330.42	139.93	495.81	635.73
Aug	Sph	159075.1	181.91	334.38	516.2931
Sep	Exp	20463.84	1082.501	1640.578	2723.078

[(1)] Power (Pow), Gaussian (Gau), Spheric (Sph), and Exponential (Exp) models. Range (R), nugget (C_0), sill (C_1), and sill variation ($C_0 + C_1$).

Table 4. Validation results

Period	Mean error	t-statistic	MSDR
		t;p-value	accuracy
Annual	-197.15	-1.2124; 0.24	1.0245
Oct	-63.78*	-2.44; 0.024	3.0368
Nov	-24.51	-0.8358; 0.41	1.6464
Dec	-57.91	-1.3996; 0.18	1.4920
Jan	38.95	0.733; 0.47	1.3805
Feb	18.04	0.3765; 0.71	2.1047
Mar	41.41	1.7892; 0.089	0.8411
Apr	9.34	0.5772; 0.57	2.0306
May	-21.93	-1.5764; 0.13	-
Jun	-7.82	-1.1415; 0.27	-
Jul	-2.20	-0.4111; 0.68	2.4263
Aug	-12.05	-2.0569; 0.056	3.1351
Sep	-26.78	-1.3677; 0.19	3.7613

* Significantly different from zero (p-value<0.05).

monthly models showed low accuracy, with MSDR values above 2 for most months. However, the annual average of long duration showed good accuracy, with an MSDR close to the unit value (1.0245). This is important because the annual average is the value most used for estimating erosivity; it is the main variable used in models for prediction of water erosion.

The months of highest rainfall, November, December, and January, showed MSDR close to 1. These months account for 52 % of annual erosivity, so it is important to have greater accuracy.

The spatial and temporal distributions of the EI_{30} for the Jaguarí River Basin are shown in figure 4.

The average annual erosivity estimated for the basin area is 7,746 MJ mm ha^{-1} h^{-1} yr^{-1}, with a standard deviation of 1,265, a minimum of 5,566, and a maximum of 11,955 MJ mm ha^{-1} h^{-1} yr^{-1}. Of this annual total, 86 % occurred between October and

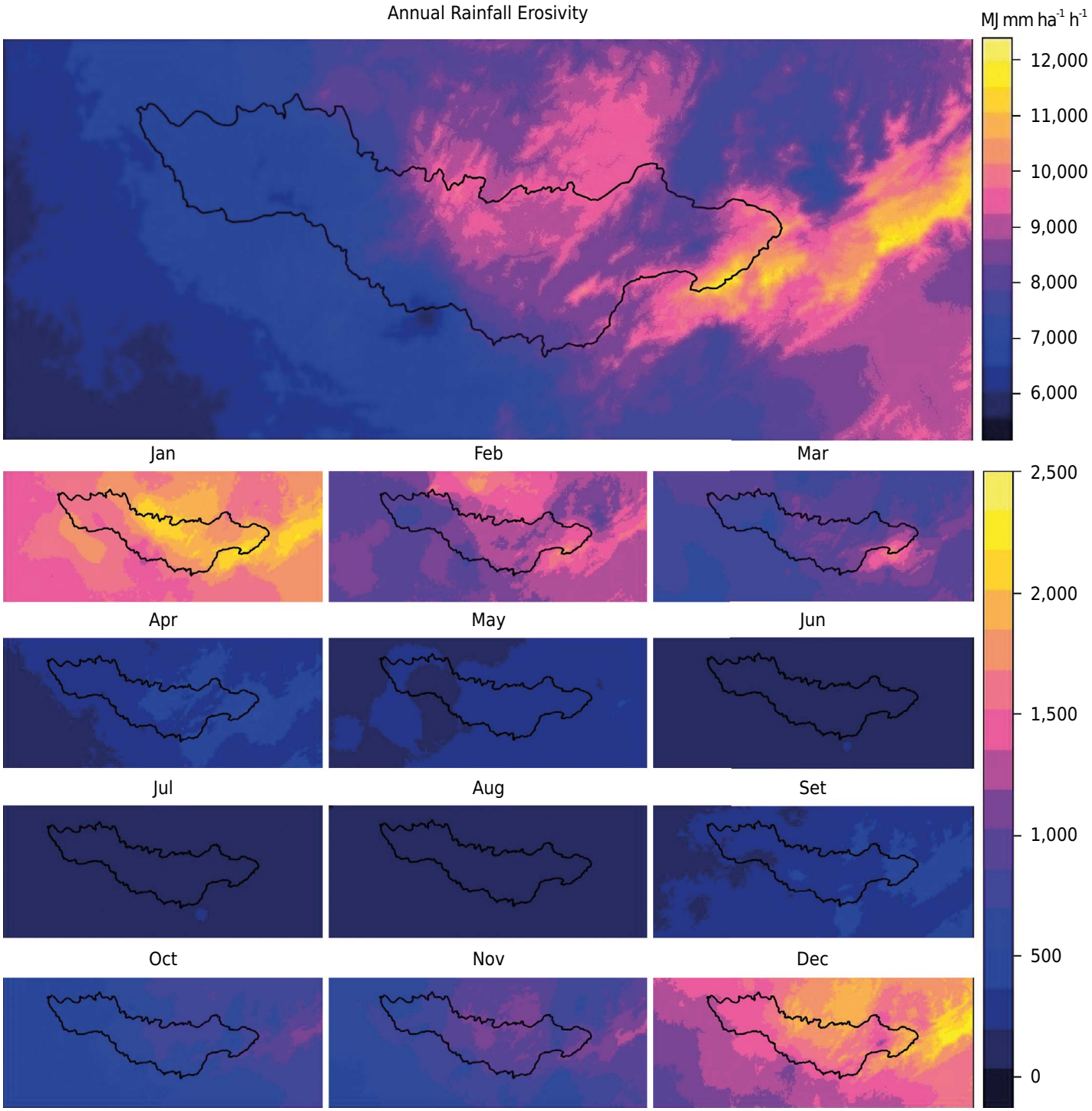

Figure 4. The EI_{30} maps (MJ mm ha^{-1} h^{-1}) for annual e monthly erosivity obtained with regression kriging in the Jaguarí River Basin.

January (Figure 4). During this period, maintenance of plant cover on the soil is essential to reduce erosive actions of the rain and, consequently, high soil losses.

The southeast region of Brazil is marked by two distinct periods in relation to rainfall: a rainy period from October to March, and a dry period from April to September. In the Jaguarí River Basin, the same pattern is observed in the data analyzed, with average monthly rainfall of 185 mm per month in the rainy period and 62 mm per month for the dry period.

In the dry period (April to August), the maximum erosivity are displaced to the south and east of the basin. Vieira and Lombardi Neto (1995) observed the same pattern for the state of São Paulo, with increased erosivity in the south region of the state during the

dry period, which may be due to the higher average rainfall in this sector of the state during the dry quarter, June-August (Prado et al., 2010).

The highest values were observed in the Mantiqueira Range region, where altitudes up to 2,066 m bring about high rainfall rates due to the orographic effect combined with the frontal (SACZ) and summer convective systems. In this region, erosivity values close to 12,000 MJ mm ha^{-1} h^{-1} yr^{-1} were estimated, in agreement with Vieira and Lombardi Neto (1995), who studied the spatial distribution of erosivity in the state of São Paulo and reported maximum values of up to 12,000 MJ mm ha^{-1} h^{-1} yr^{-1}, mainly in the Mantiqueira Range and Serra do Mar areas. Similar results and estimated values of up to 12,000 MJ mm ha^{-1} h^{-1} yr^{-1} in the state of Rio de Janeiro were reported, with the highest values in the mountain region located between latitudes of 20 and 22 °S.

Aquino et al. (2012) concluded that the erosivity of the south region of the state of Minas Gerais was considered high and strongly influenced by altitude in association with climatic characteristics. Higher erosivity is associated with higher altitude areas, such as along the Mantiqueira Range and high plateaus and mountains in the north-central part of the region. The annual erosivity values estimated by Mello et al. (2013) are also consistent with the estimates of erosivity in this study. These authors highlight the orographic effect found in mountainous regions in the southeast of Brazil, for which they reported values from 8,000 to 12,000 MJ mm ha^{-1} h^{-1} yr^{-1}.

The west portion of the basin, where the Jaguarí River flows into the Piracicaba River, shows the lowest annual and monthly values of the EI_{30}, with values above 500 MJ mm ha^{-1} h^{-1} $month^{-1}$ only for the months from November to March, a value considered critical because above this threshold, soil losses above the limit of tolerance may occur.

The study of the spatial and temporal distribution of rainfall erosivity assists conservation planning and soil and water use and management, which are of great importance in areas of intense human occupation, such as the Jaguarí River Basin. We highlight the importance of soil and water conservation efforts in the Mantiqueira Range region, where the highest values of rainfall erosivity were found, as well as the predominance of steep slopes and shallow soils very susceptible to erosive processes.

CONCLUSIONS

Rainfall erosivity in the Jaguarí River Basin shows an increasing pattern from west to east, which is related to the increase in altitude in the same direction; the highest values occurred in the vicinity of the Mantiqueira Range.

Erosivity shows a marked seasonal behavior together with the rainy period from October to March, concentrating 86 % of the estimated EI_{30} values. Monthly maximum values were up to 2,342 MJ mm ha^{-1} h^{-1} $month^{-1}$ from December to January, and there was a minimum value of 34 MJ mm ha^{-1} h^{-1} $month^{-1}$ in August.

Principal Component Analysis, together with stepwise multiple linear regression, allows simplification of the regression models obtained without losing accuracy (R^2). Regression kriging resulted in non-skewed values, good accuracy, and accuracy in prediction of average annual erosivity for the Jaguarí River Basin.

ACKNOWLEDGEMENTS

This research was funded in part by Coordination of Superior Level Staff Improvement – CAPES, the National Counsel of Technological and Scientific Development– CNPq (Process No. 305010/2013-1), and Minas Gerais State Research Foundation – FAPEMIG (Process No. CAG-APQ 01053-15).

REFERENCES

Akkala A, Devabhaktuni V, Kumar A. Interpolation techniques and associated software for environmental data. Environ Prog Sustain. 2010;29:134-41. https://doi.org/10.1002/ep.10455

Alvares CA, Stape JL, Sentelhas PC, Gonçalves JLM, Sparovek G. Köppen's climate classification map for Brazil. Meteorol Z. 2013;22:711-28. https://doi.org/10.1127/0941-2948/2013/0507

Aquino RF, Silva MLN, Freitas DAF, Curi N, Mello CR, Avanzi JC. Spatial variability of the rainfall erosivity in Southern region of Minas Gerais State, Brazil. Cienc agrotec. 2012;36:533-42. http://doi.org/10.1590/S1413-70542012000500006

Coelho CAS, Cardoso DHF, Firpo MAF. Precipitation diagnostics of an exceptionally dry event in São Paulo, Brazil. Theor Appl Climatol. 2016;125:769-84. https://doi.org/10.1007/s00704-015-1540-9

Conrad O, Bechtel B, Bock M, Dietrich H, Fischer E, Gerlitz L, Wehberg J, Wichmann V, Böhner J. System for automated geoscientific analyses (SAGA) v. 2.1.4. Geosci Model Dev. 2015;8:1991-2007. https://doi.org/10.5194/gmd-8-1991-2015

Hengl T. A practical guide to geostatistical mapping of environmental variables. Ispra:European Commission; 2007.

Hengl T, Heuvelink GBM, Rossiter DG. About regression-kriging: from equations to case studies. Comput GeoscI. 2007;33:1301-15. https://doi.org/10.1016/j.cageo.2007.05.001

Hengl T, Heuvelink GBM, Stein A. A generic framework for spatial prediction of soil variables based on regression-kriging. Geoderma. 2004;120:75-93. https://doi.org/10.1016/j.geoderma.2003.08.018

Hengl T, Rossiter DG, Stein A. Soil sampling strategies for spatial prediction by correlation with auxiliary maps. Aust J Soil Res. 2003;41:1403-22. https://doi.org/10.1071/SR03005

Lark RM. Towards soil geostatistics. Spat Stat. 2012;1:92-9. https://doi.org/10.1016/j.spasta.2012.02.001

Lombardi Neto F, Moldenhauer WC. Erosividade da chuva: sua distribuição e relação com as perdas de solo em Campinas (SP). Bragantia. 1992;51:189-96. http://doi.org/10.1590/S0006-87051992000200009

Martins SG, Avanzi JC, Silva MLN, Curi N, Norton LD, Fonseca S. Rainfall erosivity and rainfall return period in the experimental watershed of Aracruz, in the coastal plain of Espírito Santo, Brazil. Rev Bras Cienc Solo. 2010;34:999-1004. http://doi.org/10.1590/S0100-06832010000300042

Mello CR, Silva AM. Modelagem estatística da precipitação mensal e anual e no período seco para o estado de Minas Gerais. Rev Bras Eng Agr Amb. 2009;13:68-74. http://doi.org/10.1590/S1415-43662009000100010

Mello CR, Viola MR, Beskow S, Norton LD. Multivariate models for annual rainfall erosivity in Brazil. Geoderma. 2013;202-203:88-102. https://doi.org/10.1016/j.geoderma.2013.03.009

Mello CR, Sá MAC, Curi N, Mello JM, Viola MR, Silva AM. Erosividade mensal e anual da chuva no Estado de Minas Gerais. Pesq Agropec Bras. 2007;42:537-45. http://doi.org/10.1590/S0100-204X2007000400012

Meusburger K, Steel A, Panagos P, Montanarella L, Alewell C. Spatial and temporal variability of rainfall erosivity factor for Switzerland. Hydrol Earth Syst Sc. 2012;16:167-77. https://doi.org/10.5194/hess-16-167-2012

Michiels P, Gabriels D, Hartmann R. Using the seasonal and temporal precipitation concentration index for characterizing the monthly rainfall distribution in Spain. Catena. 1992;19:43-58. https://doi.org/10.1016/0341-8162(92)90016-5

Moreira MC, Cecílio RA, Pinto FAC, Pruski FF. Desenvolvimento e análise de uma rede neural artificial para estimativa da erosividade da chuva para o Estado de São Paulo. Rev Bras Cienc Solo. 2006;30:1069-76. http://doi.org/10.1590/S0100-06832006000600016

Moreira MC, Pruski FF, Oliveira TEC, Pinto FAC, Silva DD. *NetErosividade MG*: erosividade da chuva em Minas Gerais. Rev Bras Cienc Solo. 2008;32:1349-53. http://doi.org/10.1590/S0100-06832008000300042

Oliveira PTS, Wendland E, Nearing MA. Rainfall erosivity in Brazil: a review. Catena. 2012;100:139-47. https://doi.org/10.1016/j.catena.2012.08.006

Oliver JE. Monthly precipitation distribution: a comparative index. Professional Geographer. 1980;32:300-9. http://doi.org/10.1111/j.0033-0124.1980.00300.x

Oliver MA, Webster R. A tutorial guide to geostatistics: computing and modelling variograms and kriging. Catena. 2014;113:56-69. https://doi.org/10.1016/j.catena.2013.09.006

Panagos P, Ballabio C, Borrelli P, Meusburger K, Klik A, Rousseva S, Tadić MP, Michaelides S, Hrabalíková M, Olsen P, Aalto J, Lakatos M, Rymszewicz A, Dumitrescu A, Beguería S, Alewell C. Rainfall erosivity in Europe. Sci Total Environ. 2015;511:801-14. https://doi.org/10.1016/j.scitotenv.2015.01.008

Panagos P, Meusburger K, Ballabio C, Borrelli P, Alewell C. Soil erodibility in Europe: a high-resolution dataset based on LUCAS. Sci Total Environ. 2014;479-480:189-200. https://doi.org/10.1016/j.scitotenv.2014.02.010

Prado LF, Pereira Filho AJ, Xavier TMBS. Variabilidade espaço-temporal dos quantis de precipitação no Estado de São Paulo durante o verão no período de 1901 a 2007. In: Anais do XVI Congresso Brasileiro de Meteorologia: A Amazônia e o clima global; 2010; Belém. Rio de Janeiro: Sociedade Brasileira de Meteorologia; 2010.

Renard KG, Foster GR, Weesies GA, Mccool DK, Yoder DC. Predicting soil erosion by water: a guide to conservation planning with the Revised Universal Soil Loss Equation (RUSLE). Washington, DC: USDA Agriculture Handbook No 703; 1997.

Ribeiro Junior PJ, Diggle PJ. geoR: analysis of geostatistical data. R package version 1.7-5.1; 2015 [accessed on 15 Jan 2017]. Available at: https://CRAN.R-project.org/package=geoR

Silva AM. Rainfall erosivity map for Brazil. Catena. 2004;57:251-9. https://doi.org/10.1016/j.catena.2003.11.006

Silva MA, Silva MLN, Curi N, Santos GR, Marques JJGSM, Menezes MD, Leite FP. Avaliação e espacialização da erosividade da chuva no Vale do Rio Doce, região centro-leste do estado de Minas Gerais. Rev Bras Cienc Solo. 2010;34:1029-39. http://doi.org/10.1590/S0100-06832010000400003

Telles TS, Guimarães MF, Dechen SCF. The costs of soil erosion. Rev Bras Cienc Solo. 2011;35:287-98. http://doi.org/10.1590/S0100-06832011000200001

Vieira SR, Lombardi Neto F. Variabilidade espacial do potencial de erosão das chuvas do estado de São Paulo. Bragantia. 1995;54:405-12. http://doi.org/10.1590/S0006-87051995000200019

Wischmeier WH. A rainfall erosion index for a universal soil loss equation. Soil Sci Soc Am J; 1959;23:246-9. http://doi.org/10.2136/sssaj1959.03615995002300030027x

Wischmeier WH, Smith DD. Predicting rainfall erosion losses: a guide to conservation planning. Washington, DC: USDA; 1978. (Agricultural Handbook, 537).